Molecular simulation study of effect of molecular association on vapor-liquid interfacial properties

Jayant K. Singh and David A. Kofke
Department of Chemical and Biological Engineering, University at Buffalo, The State University of New York, Buffalo, New York 14260-4200

(Received 2 July 2004; accepted 26 August 2004)

Vapor-liquid interfacial properties of square-well associating fluids are studied via transition-matrix Monte Carlo simulation. Results for one-site and two-site association models are presented. Coexistence properties, surface tension, cluster distribution, density profile, and orientation profile are presented. Molecular association affects the interfacial properties and cluster fractions more than it affects the bulk densities. We observe that the surface tension exhibits a maximum with respect to association strength. This behavior is in agreement with the recent study of Peery and Evans [J. Chem. Phys. **114**, 2387 (2001)] for one site system using a square-gradient approach. © *2004 American Institute of Physics.* [DOI: 10.1063/1.1808118]

I. INTRODUCTION

A key characteristic of associating fluids is the presence of strong, short-ranged, and orientationally dependent attractive forces between molecules. Such fluids can form clusters and ordered structures even at low density. For example, hydrogen fluoride (HF) molecules are known to form linear and cyclic chain structures in the vapor phase, which can be in equilibrium with a liquid phase consisting mainly of long chains;[1,2] this phenomenon is largely responsible for the many thermodynamic anomalies exhibited by HF. Molecular association generally has a strong impact on thermodynamic behavior, and understanding of these effects is important to many applications. Hence modeling of associating fluids has been an active field of research for several decades.

Success in modeling associating fluids first came via thermodynamic methods[3] that treat association as a type of chemical bond to which chemical equilibrium thermodynamics could be applied. These approaches have been effective at producing models that can correlate the bulk-phase behavior of associating fluids. More recently modeling approaches have placed a larger emphasis on molecular-level modeling. One of the most successful techniques for analysis of this behavior is thermodynamic perturbation theory[4] and its derivatives, particularly statistical associating fluid theory (SAFT).[5,6] These developments have been supported by molecular simulation studies on related systems. Thus the modeling of the bulk phases of associating fluids has a long history, and it is still expanding. Considerably less has been done to study inhomogeneous associating systems. Peery and Evans[7] reported a study of a dimerizing (one-site model) Lennard-Jones-based associating fluid using square gradient theory. A hybrid SAFT density functional theory (DFT) approach was used to obtain the interfacial properties of associative hard core Yukawa-based fluids.[8] Alejandere, Duda, and Sokolowski[9] reported the surface tension of one-site associating Lennard-Jones systems using DFT and molecular dynamics simulation. Later, they applied canonical-ensemble Monte Carlo (NVT-MC) simulation to obtain the surface tension of associating Lennard-Jones and associating hard-core Yukuwa systems.[10] Recently we reported[11] the interfacial properties of square-well based associating fluids, with results for one-site associating square-well systems. In that work we showed the effectiveness of transition-matrix Monte Carlo (TMMC) to calculate surface tension and phase coexistence values for associating systems.

In the present study we examine the interfacial properties of two-site models. This is a significant extension, as it allows for the formation of chains of associating molecules, instead of just the dimer structures allowed by the one-site model. Our focus is on the surface tension and other interfacial properties, but in the course of obtaining these data we also must determine the vapor-liquid coexistence behavior and related bulk properties, and we report these too. Among the properties we study are monomer fraction and other cluster statistics in bulk phases, as well as density and orientation profiles across the interface. We work with simple models to see if they contain the essential features needed to reproduce the most important qualitative behaviors observed in real associating fluids. If so, these models can act as reference systems in studies of more realistic models, and can guide intuition.

The rest of this paper is organized as follows. The following section outlines the potential model and the methods used in this study. Section III presents the details of the simulations. Section IV presents the results of our studies, and we conclude in Section V.

II. MODEL AND METHODS

We study a variant of a model developed in early work on associating fluids,[6] and it is depicted in Fig. 1. A square-well contribution describes the isotropic van der Waals interaction. In real molecules, association occurs when the molecules are in close proximity and association sites are appropriately oriented. These features are represented in the potential model through an additional orientation-dependent square-well contribution. Thus the complete potential is

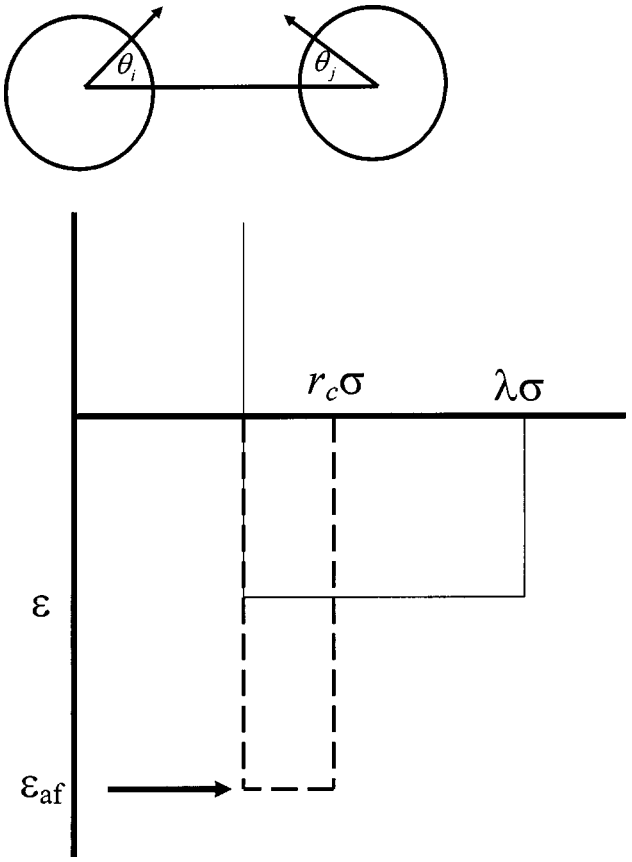

FIG. 1. Illustration of the model studied in this work.

$$u(r_{ij},\theta_i,\theta_j)=\begin{cases}\infty, & 0<r_{ij}<\sigma\\ u_{af} & \sigma\leqslant r_{ij}<r_c\sigma\\ -\epsilon, & r_c\sigma\leqslant r_{ij}<\lambda\sigma\\ 0, & r_{ij}\geqslant\lambda\sigma\end{cases},$$

$$u_{af}(r_{ij},\theta_i,\theta_j)=\begin{cases}-\epsilon_{af} & \text{if } \theta_i<\theta_c \text{ and } \theta_j<\theta_c\\ -\epsilon, & \text{otherwise,}\end{cases}$$

where θ_i and θ_j are angles between the center-to-center vector and the direction vectors on the respective atoms i and j (see Fig. 1), ϵ_{af} is the well depth of the association cone, $\lambda\sigma$ is the square-well potential diameter, ϵ is the depth of the isotropic well, and σ is the diameter of the hard core. We adopt units such that σ and ϵ are unity. In this study we use $\theta_c=27°$, $\lambda=1.5$ and $r_c=1.05$. For these parameters, in the one-site associating system, we observe that the largest cluster that can be formed is a dimer. The two-site model uses the same form for the association contribution, but applies it to two association sites, meaning there are two ranges of relative orientation for which the potential interaction is ϵ_{af}. These sites are indistinguishable, and permit the formation of more complex structures, in particular chains and rings. The second site is placed at a specific angle from the first site, and as part of this study we examined the effect of this angle on the properties—we studied angles of 90°, 120°, 160°, and 180°. We have found that this angle does not have a large effect on the properties, so we do not include all such data; the complete results will be available elsewhere.[12] The range of association energy considered here for the two-site model is $\epsilon_{af}=5.0-15.0$. For the one-site model we had examined association energies up to only 8.0, and we include here additional data for this model for $\epsilon_{af}=10.0$ (and $\epsilon_{af}=15.0$ for bulk vapor-liquid equilibria but not interfacial properties).

Surface tension is calculated using grand canonical transition matrix Monte Carlo (GC-TMMC) (Refs. 13 and 14) in conjunction with Binder's formalism.[15] The method is briefly reviewed in the following section.

A. Surface tension via GC-transition matrix Monte Carlo

We use the collection of methods described by Errington for the calculation of the surface tension. A detailed description is available elsewhere,[13] but for the sake of completeness we summarize the essence of the method and its use for calculating surface tension and phase coexistence densities and pressure.

Using the formalism suggested by Binder,[15] surface tension for three-dimensional systems is given by

$$\beta\gamma_L=\frac{\beta F_L}{2L^2}=C_1\frac{1}{L^2}+C_2\frac{\ln L}{L^2}+\beta\gamma_\infty,$$

where γ_∞ is the infinite system ($L\to\infty$) interfacial tension and C_1 and C_2 are constants to be determined by regression of simulation data, and F_L is the free energy of the finite system in a cubic volume of length L. Extrapolation of F_L for increasing L is required to get the infinite-size surface tension.

Grand-canonical Monte Carlo (GCMC) simulations are used to evaluate the free energy for a given L. GCMC simulations are conducted at fixed chemical potential μ, volume V, and temperature T, and fluctuations in particle number N are monitored to construct histograms that describe the free energy as a function of density $\rho=N/V$. For subcritical temperatures a double-peak form is observed[16] for this distribution; the peaks correspond to homogeneous phases, while the trough represents the interface. The ratio of the density-probability distribution at the intermediate minimum relative to the (mutually equal) peak densities represents the interfacial free energy,[15]

$$\beta F_L=\tfrac{1}{2}(\ln\Pi^l_{N\,\max}+\ln\Pi^v_{N\,\max})-\ln\Pi_{N\,\min},$$

where Π_N is the probability to observe a system with N particles in a grand-canonical simulation when the chemical potential is at its coexistence value; "max" and "min" refer to the values of N where the probability is at an extremum, and the superscripts "l" and "v" indicate probability values for the liquid and vapor peaks, respectively (these should be equal, but we use their average to minimize effects of an imperfect equality). Histogram reweighting is used to evaluate the coexistence value of the chemical potential.[17]

Rather than applying a visited-states approach to measure the GCMC density distribution, we employ the TMMC method.[18] This approach focuses on averaging the probabilities for transitions between states of different N. The resulting matrix of average transition probabilities can then be used to evaluate a corresponding limiting probability distri-

bution for states of different N. This is the Π_N distribution discussed above. Further detail is available in the papers of Errington.[13,14]

III. SIMULATION DETAILS

The work is divided into two parts. First, we use GC-TMMC to obtain the coexistence properties and the surface tension by Binder's extrapolation technique. Then, we perform canonical-ensemble (NVT) MC simulations of a heterogeneous vapor-liquid system in a slab geometry to examine structural properties of the interface.

In the GC-TMMC simulations, trials were performed with frequency 1:1:2:7:3 for displacement, rotation, bias-displacement,[19] insert-delete, and bias-insert-delete.[11] Multiple processors (64–256) were used in which different processors were dedicated for different ranges of density. We employed the molecular simulation package ETOMICA[20] for this purpose. Bias weights were updated for every 10 millions steps. Length of the run ranged from 50 to 100 million (average) depending on the box size. Coexistence properties were calculated using a cubic box size $L=8$ (all lengths are given in units of the core diameter σ). Surface tension was calculated using the finite-size scaling method with values of box size $L=9$, 10, and 12. Critical properties were estimated from rectilinear diameter extrapolation.[21] A cell-based neighbor list[22] was applied to speed calculations.

In the NVT-MC simulations, we employed a rectangular box of dimensions L_x, L_y, and L_z such that $L_z=L_y$ and $L_x=3\times L_y$. We started with the configuration taken from the equilibrium configurations generated from the GCMC simulations, abutting vapor and liquid configurations to form a slab geometry. Simulations were performed on about 1000 particles. The system was relaxed for 5×10^6 cycles (where a cycle consists of N Monte Carlo trial moves) and the same duration was used to collect ensemble averages. Association bias moves were used in all the NVT simulations.[19]

Simulations were performed on the two-site model as described above. We calculated vapor-liquid coexistence densities and bulk-phase cluster distributions (for ϵ_{af} up to 15.0), and surface tension (for ϵ_{af} up to 10.0) and density and cluster profiles (for ϵ_{af} up to 8.0). To study the orientation behavior of the molecules, we have computed two quantities,

$$\Phi_1=\langle\cos(\theta)\rangle,$$

$$\Phi_2=\langle|\cos(\theta)|\rangle,$$

where θ is the angle formed by the site with the normal vector of the interface. The quantity Φ_1 is zero if the molecules are aligned along the interface, or if they are randomly oriented, whereas it is equal to unity if the molecules all face normal to the interface; Φ_2 averages to 0.5 for randomly oriented molecules and to zero if the molecules are aligned with the interface, so it can distinguish these two cases when Φ_1 cannot.

We also present some new data for the one-site model examined in previous work, considering $\epsilon_{af}=10.0$ and 15.0. We discuss this system first.

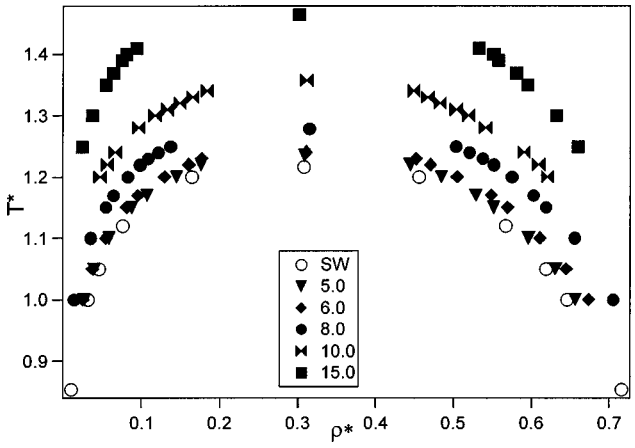

FIG. 2. Temperature-density vapor-liquid coexistence envelope of one-site square-well based associating fluids. Legend indicates values of association strength ϵ_{af}, and result labeled "SW" (where SW—spherical well) is for a nonassociating square-well model with $\lambda=1.5$. (Ref. 21) Error bars are smaller than the symbol size. Reduced units are $T^*=kT/\epsilon$, $\rho^*=\rho\sigma^3$.

IV. RESULTS AND DISCUSSION

A. One-site square-well associating systems

Figure 2 shows the coexistence densities of the one-site (dimerizing) models, for all the association energies studied in the range $\epsilon_{af}=1.0-15.0$ (including the previous data for this model[21]). The effect of association is to decrease the vapor density and increase the liquid density, while raising the critical temperature. The critical density seems to go through a maximum, in qualitative agreement with the DFT calculations of Peery and Evans;[7] however, our critical-point calculations are not rigorous, and the density variation is so small that more careful critical-point analysis might change this outcome.

Figure 3 presents the profile of overall density, monomer density, and orientation for the two association energies ϵ_{af}

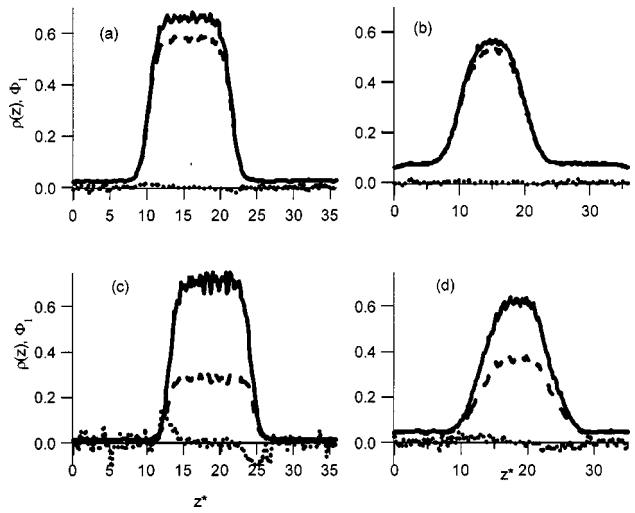

FIG. 3. Profile of overall density (solid line), monomer density (dashed line), and orientation parameter Φ_1 (dotted line nearer zero line) of one-site square-well based associating fluids for NVT simulations of coexisting liquid and vapor phases. Abscissa is the coordinate along the long axis of the simulation volume. (a) $\epsilon_{af}=5.0$, $T^*=1.0$; (b) $\epsilon_{af}=5.0$, $T^*=1.15$; (c) $\epsilon_{af}=8.0$, $T^*=1.0$; (d) $\epsilon_{af}=8.0$, $T^*=1.15$.

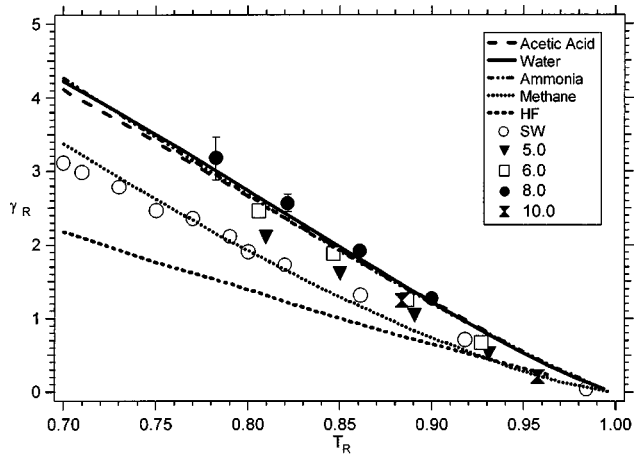

FIG. 4. Comparison of surface tension of model associating (one-site) fluids with experimental data for real fluids, (Ref. 25) as a function of temperature. Legend indicates values of association strength ϵ_{af}, and result labeled "SW" is for a nonassociating square-well model with $\lambda=1.5$. (Ref. 21) Values are reduced by critical properties: $\gamma_R=\gamma\rho_c^{1/3}/P_c$ and $T_R=T/T_c$. Error bars (where not visible) are smaller than the symbol size.

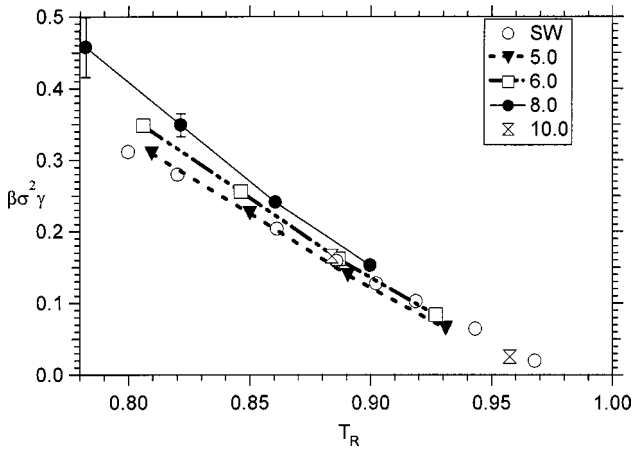

FIG. 5. Surface tension ($\gamma_R=\beta\sigma^2\gamma$) of model associating (one-site) fluids as a function of reduced temperature ($T_R=T/T_c$). Legend indicates values of association strength ϵ_{af}, and result labeled "SW" is for a nonassociating square-well model with $\lambda=1.5$. (Ref. 21) Error bars (where not visible) are smaller than the symbol size.

$=5.0$ and 8.0 at two temperatures $T=1.0$ and 1.15. At lower temperature, the vapor-liquid profile is relatively sharp. As temperature increases, the profiles become broader, as expected. Density-functional theory for a Lennard-Jones based associating one-site model indicates a small accumulation of monomer at the interface,[9] but this effect, if it exists, is too small to observe in our data.

Figure 3 also plots the orientation index Φ_1 against the length of the simulation box. Molecules in the bulk phases have a uniform orientation which represents the isotropy of the orientations of the molecules. Near the interface we see in one case [Fig. 3(c)] the signature of a specific orientation of inward-facing molecules (with association sites pointing into the bulk), but this orientational preference decreases with decreasing association energy, or increasing temperature, being negligible in the other cases. In all the simulations we have observed $\Phi_2=0.5$, indicating only that we do not have a situation in which the association sites are aligned parallel to the interface.

Figure 4 presents a corresponding-states plot of surface tension, again including only the one-site model results. In our earlier study,[11] we observed that as we increase the association energy ($\epsilon_{af}=1.0-8.0$), surface tension increases. In the present study, we increase the association energy further (to $\epsilon_{af}=10.0$) and find evidence for a change in the behavior emerging, and in particular that a maximum seems to have appeared in the surface tension (for fixed reduced temperature). This behavior is consistent with the DFT calculations of Peery and Evans,[7] To compare with their results, we have plotted the values of surface tension in units $\beta\sigma^2\gamma$ against reduced temperature. The plot is given in Fig. 5. The behavior of $\beta\sigma^2\gamma$ appears to be nonmonotonic as also shown by Peery and Evans.[7] At a given reduced temperature, increasing the association energy increases the surface tension until about $\epsilon_{af}=8.0$. Further increase in the association energy reduces the surface tension as reflected by the data of $\epsilon_{af}=10.0$. Peery and Evans suggested that this reduction in the surface tension is because the difference between the coexistence densities at a given T_R decreases. However, as shown in Fig. 6, we do not see a decrease in the coexistence densities at a given T_R. It is evident that there is more than simple density difference for this change in the behavior of the surface tension.

A possible explanation for the decrease in surface tension has to do with the saturation of the association sites in both the liquid and vapor as the association strength increases. In the case where both phases are fully dimerized, the transfer of a molecule from the liquid to the surface and into the vapor does not lead, effectively, to any dissociation of the molecule from an association partner. Thus the effect giving rise to the surface excess free energy is the isotropic dispersion attractions, which is the same as that for the nonassociating fluid. Correspondingly the surface tension can be diminished to a value comparable to that in a nonassociating fluid.

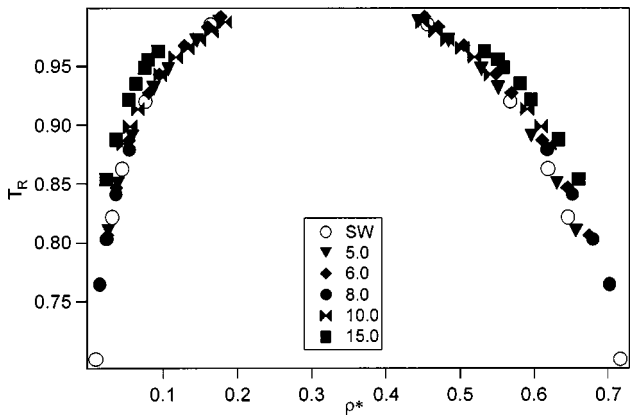

FIG. 6. Reduced temperature ($T_R=T/T_c$) vs density ($\rho^*=\rho\sigma^3$) for vapor-liquid coexistence of one-site square-well based associating fluids. Legend indicates values of association strength ϵ_{af}, and result labeled "SW" is for a nonassociating square-well model with $\lambda=1.5$. (Ref. 21) Error bars are smaller than the symbol size.

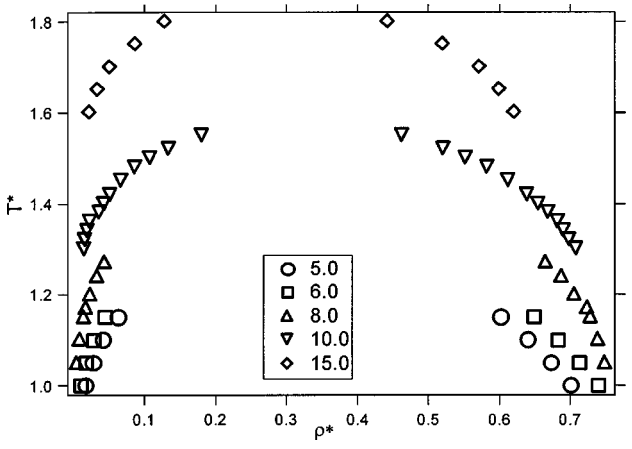

FIG. 7. Temperature-density vapor-liquid coexistence envelope of two-site square-well based associating fluids. Legend indicates values of association strength ϵ_{af}. Error bars are smaller than the symbol size. Reduced units are $T^*=kT/\epsilon$, $\rho^*=\rho\sigma^3$.

B. Two-site square-well associating systems

In this part of the study, we examine the influence of association strength on the properties of two-site models. We examine association strengths with values in the range $\epsilon_{af}=5.0-15.0$ keeping the angle between the associating sites fixed at 120°. Figure 7 presents the coexistence densities of these fluids. The behavior is not qualitatively different from the one-site fluid, i.e., the effect of increasing association energy is to decrease the vapor densities and increase the liquid densities leading to increase in the critical temperature.

Figure 8 presents the saturated vapor pressure in a Clausius-Clapeyron plot for various values of association energy. As expected, the saturation pressure decreases as the association strength increases, and no curvature is evident in any of the plots. There is a small increase (becoming more negative) in the slope of the curve with increasing association strength. We observed similar behavior in one-site associating fluids.[11]

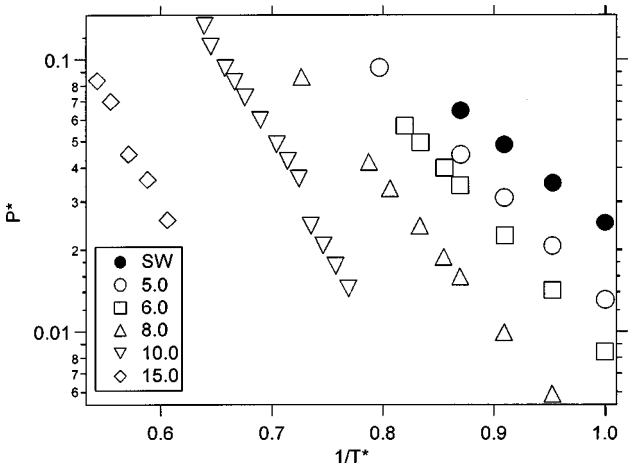

FIG. 8. Vapor pressure of the two-site associating fluids as a function of the inverse temperature. Legend indicates values of association strength ϵ_{af}; and result labeled "SW" is for a nonassociating square-well model with $\lambda=1.5$. (Ref. 21) Reduced units are $T^*=kT/\epsilon$, $P^*=P\sigma^3/\epsilon$.

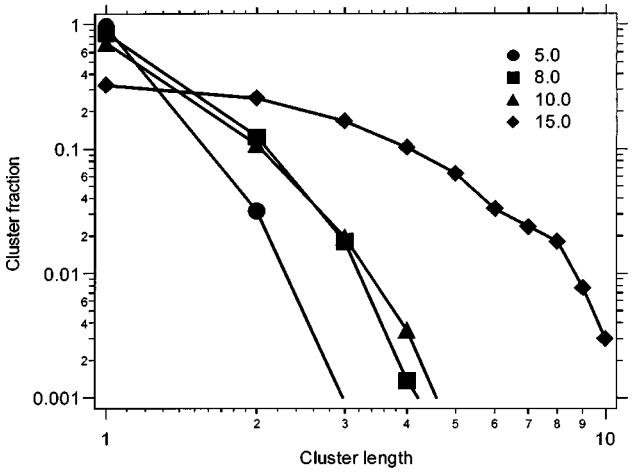

FIG. 9. Cluster fraction (number of molecules in a cluster of given size, divided by total number of molecules in phase) as a function of cluster length in the vapor phase of two-site square-well based associating fluids for a fixed reduced temperature ($T/T_c=0.89$). Legend indicates values of association strength ϵ_{af}.

Figure 9 presents the fraction of molecules in the cluster (chain) of length l in the vapor phase for various association energies at a reduced temperature of 0.89. At lower association energy ($\epsilon_{af}=5.0-10.0$), the vapor phase mainly consists of clusters of short chains ($l\leqslant 3$). There is a mild shift in the cluster distribution over this range. In comparison, the increase of association strength to 15.0 seems to bring about a more significant change in the distribution. The monomer fraction is noticeably diminished, and the distribution is flatter, with chains as long as ten having some presence. For all conditions we did not observe formation of any ring type of cluster. It is known[1] that HF forms cyclic chains in the vapor phase. Based on empirical potential models of HF,[23] the strength of association studied here is considerably less than that of HF, which would correspond to ϵ_{af} of about 25; perhaps at such large association strengths the rings would begin to be observed in the vapor phase for this model.

Figure 10 presents the fraction of molecules in the cluster of given length in the liquid phase for $\epsilon_{af}=5.0-15.0$ at a

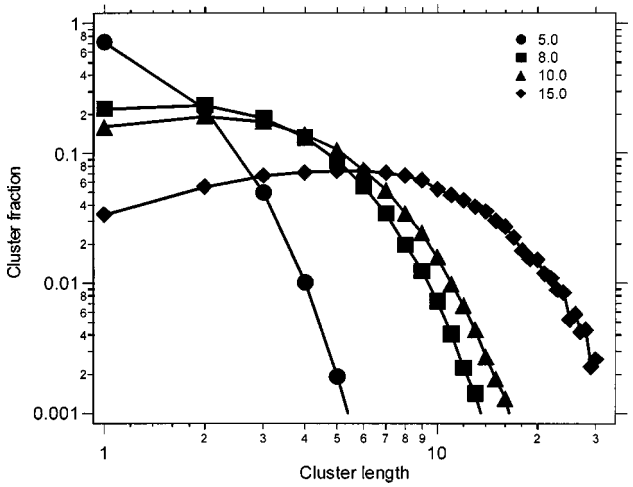

FIG. 10. Same as Fig. 9, but for liquid phase.

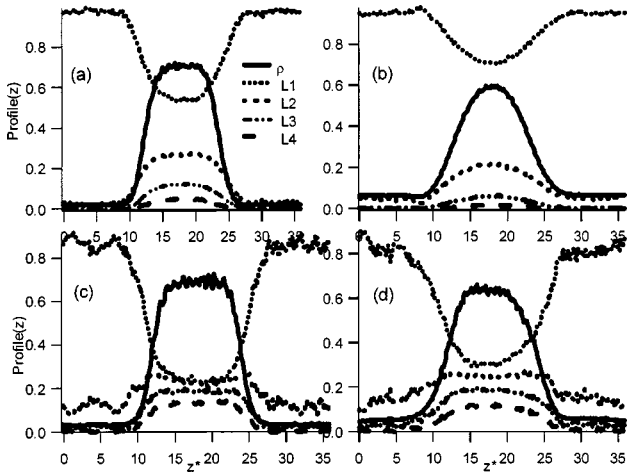

FIG. 11. Profile of overall density (solid line) and cluster fraction (number of molecules in a cluster of chain length L, divided by the total number of molecules in a local volume) (considering L from 1 to 4) of two-site square-well based associating fluids for NVT simulations of coexisting liquid and vapor phases. Abscissa is the coordinate along the long axis of the simulation volume. (a) $\epsilon_{af}=5.0$, $T^*=kT/\epsilon=1.0$; (b) $\epsilon_{af}=5.0$, $T^*=1.15$; (c) $\epsilon_{af}=8.0$, $T^*=1.2$; (d) $\epsilon_{af}=8.0$, $T^*=1.27$.

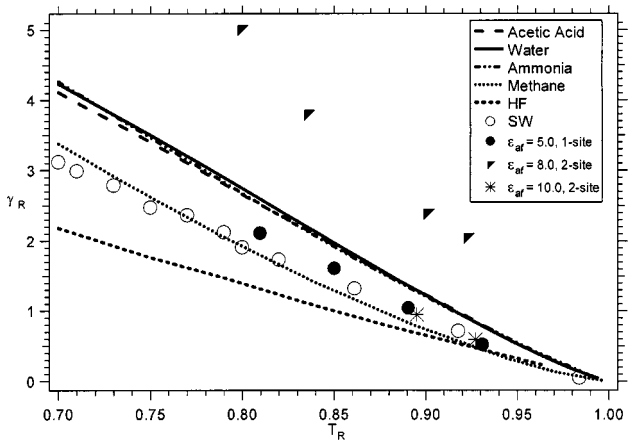

FIG. 12. Comparison of surface tension of model associating (one-site and two-site) fluids with experimental data for real fluids, (Ref. 25) as a function of temperature. Result labeled "SW" is for a nonassociating square-well model with $\lambda=1.5$. (Ref. 21) Values are reduced by critical properties: $\gamma_R=\gamma\rho_c^{1/3}/P_c$ and $T_R=T/T_c$.

reduced temperature of 0.89. Clustering of molecules in the liquid phase is significant even for $\epsilon_{af}=5.0$ where long-chain clusters are present (albeit in small amounts). The fraction of these large clusters in the liquid phase increases as the association energy increases. It is interesting to see that at higher association energy the maximum in the cluster distribution moves away from the monomer, and at the largest association strength, the peak occurs for clusters of about ten molecules. The same behavior is seen as we decrease the temperature (not shown).

Figure 11 presents the cluster profiles across the interface for different association energies at different temperatures. The results largely follow from the cluster distributions in the bulk phases, given in Figs. 9 and 10. The distributions change rather smoothly across the interface from one bulk-phase value to the other. However, there is an indication of a slight increase in the dimer fraction at the interface, noticeable at $\epsilon_{af}=8.0$ and $T^*=1.2$.

Figure 12 presents the corresponding-states plot of surface tension. We see a change in behavior between $\epsilon_{af}=8.0$ and 10.0, consistent with that observed in the one-site study, such that increasing the strength of association leads to a decrease in surface tension. It is interesting to see such a striking change even though the cluster distributions in the bulk phases of $\epsilon_{af}=8.0$ and $\epsilon_{af}=10.0$ are not very different (Figs. 9 and 10). The effect relates to phenomena particular to the surface, but the data we have gathered cannot resolve this issue. We do not have surface-tension data for larger association strengths for the two-site model, and it seems that greater association is needed to capture the experimental behavior of HF. It is difficult at such high association strengths to obtain good sampling of configurations from a simulation, because of the significant presence of long, difficult-to-break chains (chains of length even greater than 32 exist in the liquid phase for $\epsilon_{af}=15$). Simple bias moves and bias insertion of the type we have applied do not suffice for this kind of large-forming chain. A chain configurational bias method[24] might be effective in eliminating this difficulty, but we have not pursued this.

Experimental data presented in Fig. 12 indicate that there is a qualitative difference between the surface tension of associating vs nonassociating systems, and interpolation of the simulation data suggest that with the proper choice of association strength, the model can capture the behavior of the real systems (HF notwithstanding). Appropriate models for the real systems presented here would require more than two association sites on each molecule, but the data suggest that this is not such an important effect—all experimental lines (except HF) coincide with each other, and differ from the line for the nonassociating system (methane). Whether the experimental systems fall on the increasing or decreasing side of γ vs ϵ_{af} cannot be known from these data.

V. CONCLUSIONS

We have presented a study of one-site (dimer forming) and two-site (chain forming) square-well associating fluids. Phase coexistence, surface tension, profiles of overall density, cluster distribution, and molecular orientation were presented for both models. The association sites are needed in the models to describe the surface tension of real associating fluids, and these simple qualitative models are capable of capturing the variation of surface tension with temperature for a range of associating system. Simulation data provide evidence that the surface tension goes through a maximum with respect to association strength at fixed reduced temperature; this result is in accord with results from the study of dimerizing model by Peery and Evans. The two-site model should be capable of describing the hydrogen fluoride system. However, we were unable to obtain results that yield this type of agreement. This may be due in part to the failure of the model to produce associated-molecule ring structures such as are known to form in HF. Certainly more important is that we did not examine the model to a level of association

strength appropriate to the HF system. Given the observed decreasing in surface tension at higher association strengths, it seems likely that by turning the association up further, that the model could be shown to capture the anomalous low surface tension observed in HF experimentally.

ACKNOWLEDGMENTS

This work was supported by the National Science Foundation (Grant No. CTS-0219266). Computational resources have been provided by the University at Buffalo Center for Computational Research.

[1] C. Zhang, D. L. Freeman, and J. D. Doll, J. Chem. Phys. **91**, 2489 (1989); R. L. Redington, *ibid.* **75**, 4417 (1981); R. L. Redington, J. Phys. Chem. **86**, 561 (1982); **86**, 552 (1982); M. A. Suhm, Ber. Bunsenges. Phys. Chem. **99**, 1159 (1995).
[2] T. Pfleiderer, I. Waldner, H. Bertagnolli, K. Todheide, and H. E. Fischer, J. Chem. Phys. **113**, 3690 (2000); M. Deraman, J. C. Dore, J. G. Powles, J. H. Holloway, and P. Chieux, Mol. Phys. **55**, 1351 (1985).
[3] J. M. Prausnitz, R. N. Lichtenthaler, and E. G. de Azevedo, *Molecular Thermodynamics of Fluid-Phase Equilibria* (Prentice-Hall, Englewood Cliffs, 1998).
[4] M. Wertheim, J. Stat. Phys. **35**, 19 (1984); **35**, 35 (1984); **42**, 459 (1986).
[5] W. G. Chapman, K. E. Gubbins, G. Jackson, and M. Radosz, Fluid Phase Equilib. **52**, 31 (1989); Ind. Eng. Chem. Res. **29**, 1709 (1990); G. Jackson, W. G. Chapman, and K. E. Gubbins, Mol. Phys. **65**, 1 (1988); J. K. Johnson and K. E. Gubbins, *ibid.* **77**, 1033 (1992); E. Muller and K. E. Gubbins, Ind. Eng. Chem. Res. **40**, 2193 (2001); S. H. Huang and M. Radosz, *ibid.* **29**, 2284 (1990); **30**, 1994 (1991).
[6] W. G. Chapman, J. Chem. Phys. **93**, 4299 (1990).
[7] T. B. Peery and G. T. Evans, J. Chem. Phys. **114**, 2387 (2001).
[8] F. J. Blas, E. M. del Rio, E. de Miguel, and G. Jackson, Mol. Phys. **99**, 1851 (2001); G. J. Gloor, F. J. Blas, E. M. del Rio, E. de Miguel, and G. Jackson, Fluid Phase Equilib. **194–197**, 521 (2002).
[9] J. Alejandre, Y. Duda, and S. Sokolowski, J. Chem. Phys. **118**, 329 (2003).
[10] C. Tapia-Medina, P. Orea, L. Mier-y-Teran, and J. Alejandre, J. Chem. Phys. **120**, 2337 (2004).
[11] J. K. Singh and D. A. Kofke, Mol. Simul. **30**, 343 (2004).
[12] J. K. Singh, Ph.D. Dissertation, University at Buffalo, The State University at New York, 2004.
[13] J. R. Errington, Phys. Rev. E **67**, 012102 (2003).
[14] J. R. Errington, J. Chem. Phys. **119**, 3405 (2003).
[15] K. Binder, Phys. Rev. A **25**, 1699 (1982).
[16] T. L. Hill, *Thermodynamics of Small Systems, Parts I and II* (Dover, New York, 1962); W. W. Wood, J. Chem. Phys. **48**, 415 (1968).
[17] A. M. Ferrenberg and R. H. Swendsen, Phys. Rev. Lett. **61**, 2635 (1988).
[18] J.-S. Wang, T. K. Tay, and R. H. Swendsen, Phys. Rev. Lett. **82**, 476 (1999); J.-S. Wang and R. H. Swendsen, J. Stat. Phys. **106**, 245 (2002); M. Fitzgerald, R. R. Picard, and R. N. Silver, Europhys. Lett. **46**, 282 (1999); J. Stat. Phys. **98**, 321 (2000).
[19] S. Wierzchowski and D. A. Kofke, J. Chem. Phys. **114**, 8752 (2001).
[20] D. A. Kofke and B. C. Mihalick, Fluid Phase Equilib. **194–197**, 327 (2002).
[21] J. K. Singh, D. A. Kofke, and J. R. Errington, J. Chem. Phys. **119**, 3405 (2003).
[22] M. P. Allen and D. J. Tildesley, *Computer Simulation of Liquids* (Clarendon, Oxford, 1987).
[23] D. Visco and D. A. Kofke, J. Chem. Phys. **109**, 4015 (1998).
[24] J. I. Siepmann and D. Frenkel, Mol. Phys. **75**, 59 (1992).
[25] C. F. Beaton and G. F. Hewitt, *Physical Property Data for the Design Engineer* (Hemisphere, New York, 1989).